

# Author Queries

*Journal:* Proceedings of the Royal Society B






*Manuscript:* rspb20142302

As the publishing schedule is strict, please note that this might be the only stage at which you are able to thoroughly review your paper.

Please pay special attention to author names, affiliations and contact details, and figures, tables and their captions.

If you or your co-authors have an ORCID ID please supply this with your corrections. More information about ORCID can be found at <http://orcid.org/>.

No changes can be made after publication.

- Q1** Please provide volume number and page range for ref. [11]. 
- Q2** Please provide volume number for ref. [34]. 
- Q3** Reference [54] is provided in the list but is not cited in the text. Please supply citation details or delete the reference from the reference list. 
- Q4** While the online version of figure 1 will be in colour, we have been instructed to print the figure in black and white. Please note that if you have explicitly referred to colour in the caption this may affect the legibility of the figure in print. 
- SQ1** Your paper has exceeded the free page extent and will attract page charges. 



## Research

**Cite this article:** Glazier DS, Hirst AG, Atkinson D. 2015 Shape shifting predicts ontogenetic changes in metabolic scaling in diverse aquatic invertebrates. *Proc. R. Soc. B* 20142302.

<http://dx.doi.org/10.1098/rspb.2014.2302>

Received: 17 September 2014

Accepted: 6 January 2015

**Subject Areas:**

developmental biology, physiology, theoretical biology

**Keywords:**

aquatic invertebrates, body shape, metabolic scaling, ontogeny, resource-transport networks, surface area

**Author for correspondence:**

Douglas S. Glazier

e-mail: [glazier@juniata.edu](mailto:glazier@juniata.edu)

Electronic supplementary material is available at <http://dx.doi.org/10.1098/rspb.2014.2302> or via <http://rspb.royalsocietypublishing.org>.

# Shape shifting predicts ontogenetic changes in metabolic scaling in diverse aquatic invertebrates

Douglas S. Glazier<sup>1</sup>, Andrew G. Hirst<sup>2,3</sup> and David Atkinson<sup>4</sup>

<sup>1</sup>Department of Biology, Juniata College, Huntingdon, PA 16652, USA

<sup>2</sup>School of Biological and Chemical Sciences, Queen Mary University of London, London E1 4NS, UK

<sup>3</sup>Centre for Ocean Life, National Institute for Aquatic Resources, Technical University of Denmark, Kavalergården 6, Charlottenlund 2920, Denmark

<sup>4</sup>Institute of Integrative Biology, University of Liverpool, Biosciences Building, Crown St., Liverpool L69 72B, UK

Metabolism fuels all biological activities, and thus understanding its variation is fundamentally important. Much of this variation is related to body size, which is commonly believed to follow a 3/4-power scaling law. However, during ontogeny, many kinds of animals and plants show marked shifts in metabolic scaling that deviate from 3/4-power scaling predicted by general models. Here, we show that in diverse aquatic invertebrates, ontogenetic shifts in the scaling of routine metabolic rate from near isometry ( $b_R =$  scaling exponent approx. 1) to negative allometry ( $b_R < 1$ ), or the reverse, are associated with significant changes in body shape (indexed by  $b_L =$  the scaling exponent of the relationship between body mass and body length). The observed inverse correlations between  $b_R$  and  $b_L$  are predicted by metabolic scaling theory that emphasizes resource/waste fluxes across external body surfaces, but contradict theory that emphasizes resource transport through internal networks. Geometric estimates of the scaling of surface area (SA) with body mass ( $b_A$ ) further show that ontogenetic shifts in  $b_R$  and  $b_A$  are positively correlated. These results support new metabolic scaling theory based on SA influences that may be applied to ontogenetic shifts in  $b_R$  shown by many kinds of animals and plants.

## 1. Introduction

All living activities depend on metabolism for energy and materials. Therefore, understanding variation in metabolic rate is of fundamental importance in biology. Much of this variation is related to body size, but how and why these relationships occur remain vexing questions. General models assume that metabolic rate scales monotonically with body size according to the simple power function

$$R = aM^b, \quad (1.1)$$

where  $R$  is metabolic rate,  $a$  is the scaling coefficient (antilog of the intercept in a log–log plot),  $M$  is body mass and  $b$  (henceforth  $b_R$ ) is the scaling exponent (linear slope of a log–log plot that frequently approximates 3/4) [1,2]. However, metabolic scaling often shows marked shifts during ontogeny in animals and plants ( $b_R$  varying mostly between 2/3 and 1, but also showing values outside this range) [3–7] that are not well understood. These metabolic shifts are important because they appear to be fundamentally linked to other ontogenetic changes in the physiology, growth rate, cell size, body composition, behaviour and ecology of a species [3–7].

Here, we show that ontogenetic changes in body shape and associated surface area (SA)-related resource supply predict frequently observed shifts from near isometric ( $b_R \sim 1$ ) to negatively allometric ( $b_R < 1$ ) intraspecific metabolic scaling (=type III scaling [4]) in diverse aquatic invertebrates. Crucially, we also show that shape shifting predicts more rarely observed changes in metabolic

scaling that occur in the opposite direction (from shallow to steep scaling). Our results demonstrate that the prediction of metabolic scaling from the body-shape-related scaling of SA applies more widely than that recently described by Hirst *et al.* [8]. We show here that this predictive power applies to marked variation in metabolic scaling seen not only among diverse pelagic (open water) animal taxa [8], but also during the intraspecific ontogeny of both pelagic invertebrates and those that exhibit developmental shifts from pelagic to benthic (bottom-dwelling) lifestyles. A critical assumption of our shape-shifting model is that the supply of resources or loss of wastes scales with external body surface, thus implying that exchange of materials such as respiratory gases is distributed over the body surface, which we evaluate herein. We also discuss potential implications of our findings for ontogenetic shifts in metabolic scaling observed in many other kinds of animals and plants.

## 2. Theoretical background

Metabolic rate may be controlled by the supply of, or demand for, resources [9–11]. Both should be considered in order to attain a comprehensive understanding of the scaling of metabolic rate with body size [4,12,13]. Here, we test opposing predictions from influential metabolic scaling theories that focus on transport of resources and waste products such as respiratory gases between the external environment and metabolizing cells. This transport may be influenced by two major steps: the exchange of materials across body surfaces and the transport of materials through internal networks. These steps are the foci for two prominent theoretical approaches to understanding and predicting biological scaling: SA theory [4,8,14,15] and resource-transport network (RTN) theory [1,2,16,17], respectively.

Although both SA and internal transport networks may be important in influencing metabolic rate and its scaling with body size, SA theory (including widely applied DEB theory, which incorporates SA theory: see [8,18,19]) predicts that body-shape changes should have opposite effects on the metabolic scaling exponent  $b_R$  (see equation (1.1)) than those predicted by existing RTN theory [8]. If an organism shows isomorphic growth (i.e. it grows with equal proportions in all three dimensions, so as to maintain a constant shape), SA theory (based on simple Euclidean geometry) predicts that  $b_R = 2/3$ , whereas RTN theory typically predicts that  $b_R = 2/3$  [2,17] or  $3/4$  [1,2,16], depending on the physical properties of the transport network [20,21]. These predicted scaling exponents of  $2/3$  and  $3/4$  have received the most attention by biologists since the seminal studies of Rubner [14] and Kleiber [22] over 80 years ago. However, if an organism displays nearly two-dimensional growth (e.g. it grows in length and width without any significant change in depth, thus appearing increasingly flat), SA theory predicts that  $b_R \sim 1$  [8,15], whereas RTN models predict that  $b_R \sim 1/2$  [17],  $5/8$  [2,8] or  $2/3$  [16], depending on network geometry and dynamics. In addition, if an organism exhibits nearly one-dimensional growth (e.g. it grows in length without any significant change in width or depth, thus showing an increasingly elongated shape), SA theory predicts that  $b_R \sim 1$  [8,15], whereas RTN theory predicts that  $b_R \sim 0$  [17],  $1/4$  [2,8] or  $1/2$  [16], again depending on network properties. Therefore, increased elongation or flattening during ontogeny (trends towards one- or two-dimensional growth) should lead to an

increase in  $b_R$ , according to SA theory, whereas RTN theory predicts the opposite—a decrease in  $b_R$ . Conversely, ontogenetic trends away from increasingly elongated one-dimensional or flattened two-dimensional growth, but towards isomorphic three-dimensional growth reverse the changes in  $b_R$  predicted by the two theories: SA theory predicts decreasing, and RTN theory increasing  $b_R$ . Studying the effects of ontogenetic shape shifting on metabolic scaling thus provides an excellent opportunity to test the relative validity of models based on two major competing theories of metabolic scaling, which is much needed for the field to advance [23,24].

## 3. Testing theory using animals with mixed ontogenetic metabolic scaling

Several kinds of aquatic animals with complex life cycles exhibit ontogenetic shifts in the scaling of aerobic metabolism, typically measured as the rate of oxygen consumption. In these animals, respiration scaling exponents ( $b_R$ ) most often change from near 1 in larvae or young juveniles to less than 1 in older juveniles or adults [3,4,25], but reverse shifts also rarely occur [26,27]. From the literature, we collected respiratory and morphometric data on aquatic invertebrates that have complete or partial pelagic (open water) life histories to test whether and how these ontogenetic shifts in metabolic scaling are related to changes in body shape.

Unfortunately, actual measurements of body SA during ontogeny are rare [8]. Therefore, as a first-order approximation, we quantified differences in shape-related growth between life-history phases by using Euclidean geometry for smooth surfaces to deduce SA-mass scaling exponents ( $b_A$ , or the slope of  $\log_{10}$  body SA versus  $\log_{10}$  body mass). To achieve this, we first used readily available body length and mass data to obtain mass-length scaling exponents ( $b_L$ ), estimated as the slopes of least-squares regressions (LSRs) of  $\log_{10}$  body mass versus  $\log_{10}$  body length (along the longest axis). Values of  $b_L$  were calculated separately for larvae, juveniles and adults [28]. Logarithmic transformation was used to permit easy detection of proportional changes [29]. If growth is occurring proportionally in three dimensions without any change in mass density,  $b_L$  should be 3, whereas if growth involves pure elongation in only one dimension (along the longest axis) or pure flattening because of size increases in only the two longest dimensions,  $b_L$  should be 1 or 2, respectively [8]. For intermediate patterns of body-shape change, involving disproportionate growth in one or two of the longest dimensions,  $1 \leq b_L \leq 3$ . Values of  $b_L$  may even be more than 3, if growth in the shortest dimensions [width and (or) depth] is proportionately greater than that for length along the longest axis that is used to calculate  $b_L$  (i.e. the animal is becoming relatively thicker and/or broader) [8].

Ranges of  $b_A$  values were inferred from  $b_L$  values that are less than or equal to 3 by using formulae for the extreme possibilities of different degrees of elongation (one-dimensional growth) and flattening (two-dimensional growth) [8]. The formula for different degrees of elongation is

$$b_A = \frac{1}{2} \left( 1 + \frac{1}{b_L} \right), \quad (3.1)$$

whereas the formula for different degrees of flattening is

$$b_A = 2 \left( \frac{1}{b_L} \right). \quad (3.2)$$

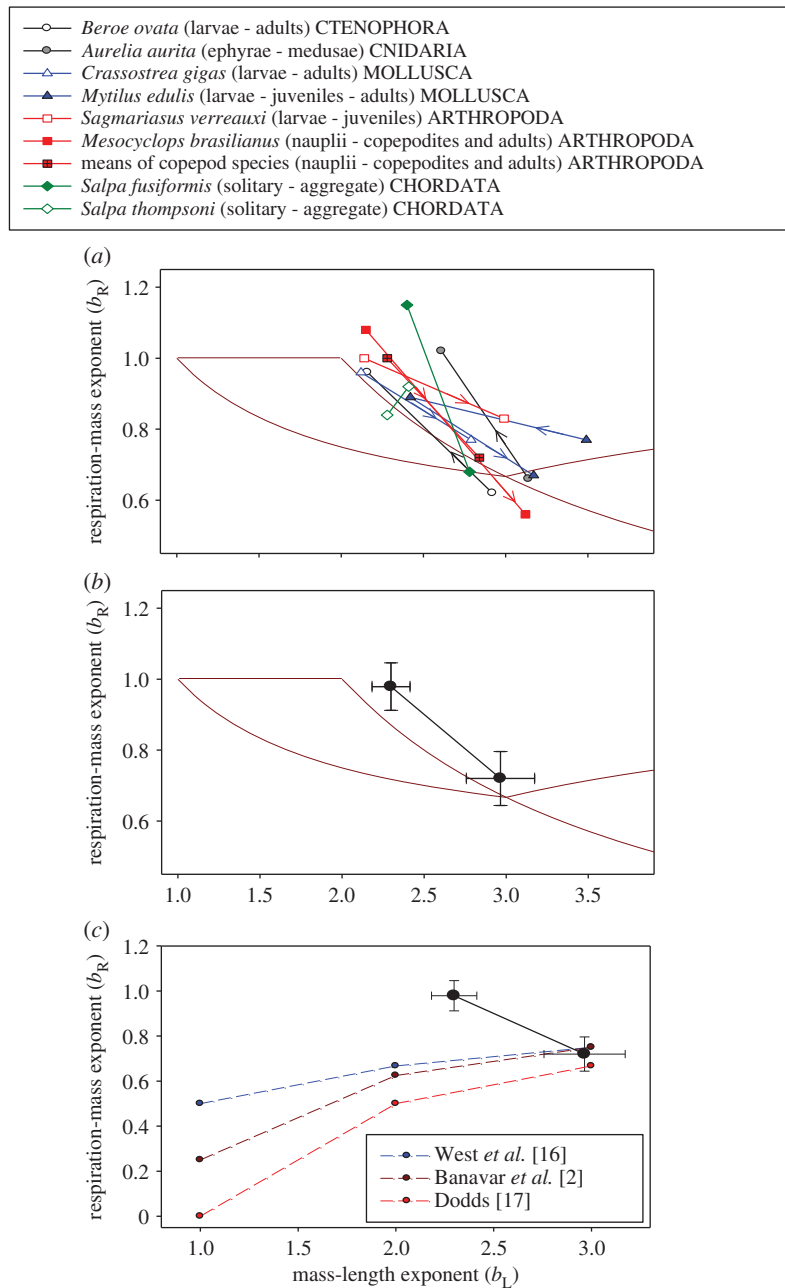


**Figure 1.** Ontogenetic shifts of respiration-mass exponents ( $b_R$ ) in relation to mass-length exponents ( $b_L$ ) of several species of aquatic invertebrates in five different phyla (a) and for all species averaged together (b,c), where  $b_R$  is the scaling exponent for  $\log_{10}$  RMR in relation to  $\log_{10}$  body mass, and  $b_L$  is the scaling exponent for  $\log_{10}$  body mass in relation to  $\log_{10}$  total body length (data from tables 1 and 2). Multiple  $b$  values for the life-history stage of a species or group of species (copepods) were averaged. Arrows indicate the direction of ontogenetic change. In (b,c), the upper left and lower right points were calculated by averaging all of the paired  $b_R$  and  $b_L$  values that occurred in ontogenetic stages with the higher versus lower  $b_R$ , respectively. The 95% confidence limits are shown for each mean value of  $b_R$  and  $b_L$ . Also shown in (b) are the bounded range of values of  $b_A$  ( $\log_{10}$  body SA in relation to  $\log_{10}$  body mass) in relation to  $b_L$  (depicted as light purple lines) calculated using equations (3.1) and (3.2) based on Euclidean geometry (also see [8]); and in (c) the predicted effects of body-shape changes ( $b_L$ ) on  $b_R$  (depicted as dashed coloured lines) according to the RTN models of West *et al.* [16], Banavar *et al.* [2] and Dodds [17] (also see [8]). Note that in seven of eight species sampled, ontogenetic shifts in  $b_L$  are accompanied by inverse shifts in  $b_R$ , as predicted by SA scaling theory (b), but in contradiction to RTN scaling theory (c). (Online version in colour.)

Equation (3.1) applies for  $1 \leq b_L \leq 3$ ; and equation (3.2) applies for  $2 \leq b_L \leq 3$ , as represented in figure 1a,b by the left- and right-hand purple curves for  $b_L \leq 3$ , respectively. Ranges of potential  $b_A$  values were also inferred from  $b_L$  values that are more than 3 by using formulae quantifying disproportionate thickening in one or two of the shortest dimensions. The formula for thickening of only the shortest dimension is the same as equation (3.2), whereas the formula for thickening of only the two shortest dimensions is the same as equation (3.1), as represented in figure 1a,b by the bottom and top purple curves for  $b_L > 3$ , respectively. When

data on the scaling of body width with body length were available, it was possible to predict a single value of  $b_A$  rather than a range (see electronic supplementary material).

The empirical  $b_L$  values and inferred  $b_A$  values were then compared to scaling exponents ( $b_R$ ) for regressions of  $\log_{10}$  routine metabolic (oxygen consumption) rate (RMR) in relation to  $\log_{10}$  body mass of different ontogenetic stages both within and among several species of aquatic invertebrates.

Both  $b_L$  and  $b_R$  values were based on LSR, the method used for all of the literature scaling analyses included in our study. An alternative, often used method, reduced major axis (RMA)

190 analysis, gave similar  $b$  values ( $b_{\text{RMA}} = b_{\text{LSR}}/r$ ) to those from  
 191 LSR, because reported correlation coefficients ( $r$ ) were always  
 192 high (more than or equal to 0.8). The  $r$  values for  $b_L$  averaged  
 193  $0.97 \pm 0.01$  ( $\pm 1$  s.e.,  $n = 15$ ), and those for  $b_R$  averaged  $0.96 \pm$   
 194  $0.01$  ( $n = 19$ ) (calculated from  $r^2$  values in the electronic sup-  
 195 plementary material for table 1). As a result,  $b_L$  and  $b_R$   
 196 values based on RMA analyses averaged only approximately  
 197 3–4% higher than those based on LSR.

## 4. Results

202 We compared conspecific  $b_L$ ,  $b_R$  and inferred  $b_A$  values for differ-  
 203 ent ontogenetic phases of a ctenophore, a scyphozoan, two  
 204 bivalves, two crustaceans and two thaliaceans (table 1), as well  
 205 as mean heterospecific values for the nauplii, copepodites and  
 206 adults of several copepod crustaceans (table 2).

207 For seven of the eight species sampled, ontogenetic shifts  
 208 in the metabolic scaling exponent ( $b_R$ ) are accompanied by  
 209 inverse shifts in the scaling exponent of body mass in relation  
 210 to length ( $b_L$ ) (table 1 and figure 1a). The only exception is the  
 211 pelagic tunicate *Salpa thompsoni*, which showed no significant  
 212 difference in  $b_R$  or  $b_L$  between the solitary (oozoid) and aggre-  
 213 gate (blastozoid) life cycle stages (table 1 and figure 1a).  
 214 Remarkably, even this exception supports a link between  $b_R$   
 215 and  $b_L$ , because both life stages of *S. thompsoni* have relatively  
 216 high  $b_R$  values associated with relatively low  $b_L$  values, as com-  
 217 pared with the exponents exhibited by the other species  
 218 sampled (figure 1a). Furthermore, inverse shifts in  $b_R$  and  $b_L$   
 219 occurred in the other seven species sampled regardless of  
 220 whether  $b_R$  showed an increase or decrease during ontogeny  
 221 (table 1 and figure 1a). Inverse relationships between  $b_R$  and  
 222  $b_L$ , also seen among all of the species averaged together  
 223 (figure 1b,c), follow SA theory (figure 1b), but contradict all  
 224 existing RTN models (figure 1c). Although ontogenetic  
 225 stages with a mean  $b_L \sim 3$  ( $2.97 \pm 0.21$  95% confidence interval  
 226 (CI)) exhibited a mean  $b_R$  ( $0.72 \pm 0.08$ ) not significantly differ-  
 227 ent from  $2/3$  or  $3/4$ , as predicted by both SA and RTN theory,  
 228 stages with a mean  $b_L \sim 2.3$  ( $2.30 \pm 0.12$ ) exhibited a mean  $b_R$   
 229 ( $0.98 \pm 0.07$ ) not significantly different from 1 and signifi-  
 230 cantly greater than  $2/3$  and  $3/4$ , as predicted by SA theory,  
 231 but in contradiction to all RTN models, which predict  $b_R$   
 232 values less than  $2/3$  or  $3/4$  (figure 1b,c).

233 As the scaling exponent for body SA ( $b_A$ ), as inferred from  
 234 Euclidean geometry, is inversely related to  $b_L$  (figure 1a; and  
 235 equations (3.1) and (3.2)), it follows mathematically that onto-  
 236 genetic shifts in  $b_R$  and  $b_A$  should be positively correlated, as  
 237 observed in seven of the eight species sampled (table 1 and  
 238 figure 2a). As predicted by SA theory,  $b_R$  and  $b_A$  are also posi-  
 239 tively correlated for all species averaged together (figure 2b),  
 240 and when these exponents were compared pairwise among  
 241 each of the ontogenetic phases of each species (figure 2c).  
 242 The slope for the latter correlation (1.14) is not significantly  
 243 different from 1, as expected if  $b_R$  varied in direct proportion  
 244 to  $b_A$  (figure 2c).

245 Similar ontogenetic shifts are seen when  $b_R$ ,  $b_L$  and  $b_A$   
 246 values are compared between nauplii and copepodites/  
 247 adults averaged among several species of copepods (table 2  
 248 and figure 1a). The heterospecific, inversely related shifts in  
 249  $b_R$  and  $b_L$  almost exactly parallel those observed for the  
 250 single copepod species *Mesocyclops brasiliensis* (figure 1a).

251 The spiny lobster *Sagmariasus verreauxi* nicely exemplifies  
 252 how ontogenetic changes in metabolic rate and body shape

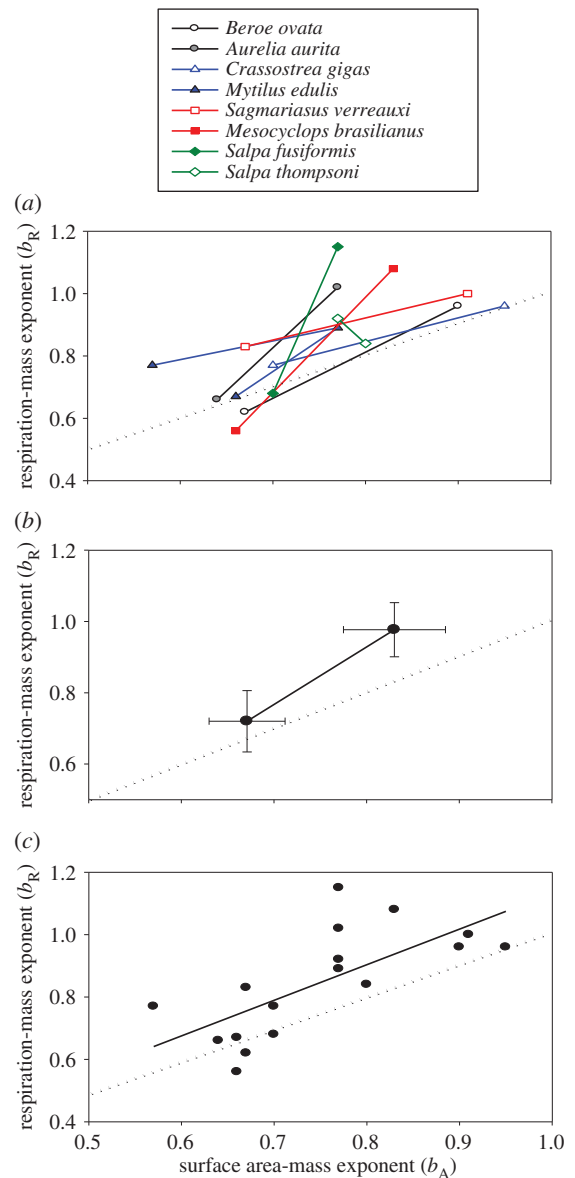


**Figure 2.** Ontogenetic shifts of respiration-mass exponents ( $b_R$ ) in relation to SA-mass exponents ( $b_A$ ) of several species of aquatic invertebrates (a) and for all species averaged together (b), where  $b_R$  is the scaling exponent for  $\log_{10}$  RMR in relation to  $\log_{10}$  body mass, and  $b_A$  is the scaling exponent for  $\log_{10}$  body mass in relation to  $\log_{10}$  total body length (data from table 1). Values of  $b_A$  were calculated using  $b_L$  values and additional data in the electronic supplementary material. Multiple  $b_R$  values for the life-history stage of a species were averaged, whereas the midpoint was used when only a range of  $b_A$  values was available. In (b), the lower left and upper right points were calculated by averaging all of the paired  $b_R$  and  $b_A$  values that occurred in ontogenetic stages with the lower versus higher  $b_R$ , respectively. The 95% confidence limits are shown for each mean value of  $b_R$  and  $b_A$ . As predicted by SA scaling theory (also see [8]), in seven of eight species sampled, ontogenetic shifts in  $b_A$  are accompanied by positively correlated shifts in  $b_R$ . Also shown in (c) is a significant positive correlation between  $b_R$  and  $b_A$  for each ontogenetic stage of each species. The equation for the LSR line is:  $b_R = 1.14 \pm 0.64$  95% CI ( $b_A$ ) - 0.0092 ( $r^2 = 0.454$ ;  $p = 0.0018$ ,  $n = 17$ ). In (a-c), the dotted diagonal lines represent  $b_R = b_A$ . (Online version in colour.)

correlate. The phyllosoma larvae are very thin and flat and show nearly two-dimensional growth, until they metamorphose into adult-looking benthic juveniles that are much thicker and show three-dimensional growth. This marked shift in growth pattern and body form is represented by an abrupt ontogenetic shift in  $b_L$  values: from  $2.142 \pm 0.260$

(95% CI) in the phyllosoma larvae to  $2.991 \pm 0.037$  in the juveniles (figure 3a and table 1). The phyllosoma  $b_L$  value is not significantly different from 2, whereas the juvenile  $b_L$  value is not significantly different from 3. As a result, the scaling exponents predicted for SA ( $b_A$ ) from Euclidean geometry (see the electronic supplementary material) are 0.91 for the phyllosomas and 0.67 for the juveniles (table 1). Like  $b_A$ , the  $b_R$  values for RMR are also higher in the phyllosomas ( $1.002 \pm 0.081$ ) than in the juveniles ( $0.829 \pm 0.157$ ) (figure 3b and table 1). Comparisons of the 95% CI [20,29] reveal that the  $b_L$  and  $b_R$  values are both significantly different between the two life-history stages. The phyllosoma  $b_R$  value is not significantly different from 1, but is significantly greater than 1/2, 5/8, 2/3 and 3/4. By contrast, the juvenile  $b_R$  value is significantly less than 1, not significantly different from 3/4, and significantly greater than 1/2, 5/8 and just barely 2/3.

## 5. Discussion

The parallel changes in the scaling exponents for RMR and inferred SA observed in seven of the eight species sampled supports the importance of SA changes in the observed ontogenetic shifts in metabolic scaling, but contradicts predictions of all current models emphasizing internal RTNs. SA theory predicts positive correlations between the scaling exponents for SA ( $b_A$ ) and RMR ( $b_R$ ), as observed, whereas current RTN theory incorrectly predicts negative correlations between  $b_A$  and  $b_R$ . Although RTN theory has been claimed to be universally applicable to all of life [1,16] or at least to macroscopic multicellular eukaryotes [32], RTN theory may not apply to animals without circulatory systems or with open or incompletely closed circulatory systems [2,4,21], which are far more common taxonomically than those with completely closed circulatory systems (including only vertebrates, cephalopod molluscs, and some annelid and nemertean worms [33,34]). In fact, two of the animal species included in our study have no or very rudimentary circulatory systems (a ctenophore and scyphozoan), whereas the other six have open or incompletely closed circulatory systems (the bivalve, crustacean and thaliacean species) [34]. Nevertheless, Hirst *et al.* [8] have shown that the similarly steep ontogenetic scaling of both metabolic rate and SA with body mass in squids (cephalopods), which have closed circulatory systems, is also consistent with SA theory, but not with RTN theory. This additional deviation from RTN theory may be because squids use both their skin and gills for gas exchange and also distribute resource-laden blood by means of multiple hearts found throughout the body [34], rather than from a single centralized heart or distribution centre, as assumed by the theory [1,2,16,17]. If current RTN theory does not apply to squids for these reasons, then annelid worms that use multiple hearts to pump blood [33] and nemertean worms that have no heart at all [34] may also be exceptions. Therefore, current RTN theory appears to apply to only a small subset of animals: perhaps only vertebrates with single central hearts in a completely closed vascular system. Even the application of RTN theory to vertebrates may be of limited use, because currently it cannot explain large variation in the metabolic scaling exponent observed in various vertebrate classes that appears to be related to physiological state, ecological lifestyle or environmental

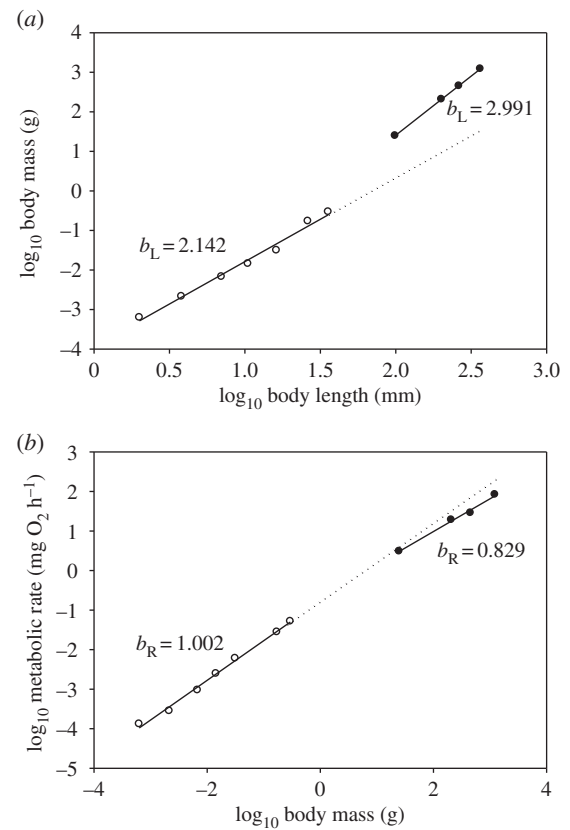


**Figure 3.** Scaling of  $\log_{10}$  wet body mass in relation to  $\log_{10}$  total body length (a) and  $\log_{10}$  RMR in relation to  $\log_{10}$  wet body mass (b) in phyllosoma larvae (open points) and juveniles (filled points) of the spiny lobster *S. verreauxi* maintained at 21–23°C. Each point in (a,b) is based on 4–11 replicate measurements, respectively [30,31]. The phyllosoma points represent instars 1, 3, 6, 9, 12, 15 and 17. The standard errors for each RMR value are all less than 20% of the mean. The LSR equations for the scaling lines and their coefficients of determination ( $r^2$ ) and significance levels ( $p$ ) for phyllosoma larvae and juveniles are: (a)  $Y = -3.931 + 2.142 (X)$ ,  $r^2 = 0.988$ ,  $p = 0.00001$ ;  $Y = -4.574 + 2.991 (X)$ ,  $r^2 = 1.000$ ,  $p < 0.00001$ ; and (b)  $Y = -0.773 + 1.002 (X)$ ,  $r^2 = 0.995$ ,  $p < 0.00001$ ;  $Y = -0.673 + 0.829 (X)$ ,  $r^2 = 0.993$ ,  $p = 0.00353$ , respectively. The number by each line is the scaling slope (exponent). Linear extrapolations of the empirical scaling lines for the phyllosoma larvae are shown as dotted lines to highlight the ontogenetic scaling shifts for both body shape (a) and metabolic rate (b).

conditions [12,35–38]. Perhaps next-generation resource exchange and supply theory may resolve these problems (also see §6).

In any case, the positive associations between  $b_A$  and  $b_R$  observed in this study are remarkable because they occur in animals with very different body designs, including five different phyla, and furthermore, they occur regardless of whether  $b_A$  increases, or decreases, during ontogeny. Therefore, it is unlikely that these correlations are merely side effects of  $b_A$  and  $b_R$  being independently related to other unmeasured factors associated with developmental maturation or ontogenetic age. Rather, it is more likely that shape shifting directly affects metabolic scaling via changes in SA available for resource uptake and waste excretion.

This hypothetical mechanism for how shape shifting may affect metabolic scaling seems especially applicable to the thin-skinned pelagic animals (larval or adult) that we have studied here and in a related paper [8]. Phyllosoma, veliger and other pelagic larvae of many marine animals that show

**Table 1.** Ontogenetic scaling exponents from LSRs of  $\log_{10}$  body mass in relation to  $\log_{10}$  body length ( $b_L$ ) and  $\log_{10}$  RMR in relation to  $\log_{10}$  body mass ( $b_R$ ) for larvae, juveniles and (or) adults of the Atlantic ctenophore *Beroe ovata*, moon jellyfish *A. aurita*, Pacific oyster *C. gigas*, common mussel *M. edulis* and spiny lobster *S. verreauxi*; for nauplii, copepodites and adults of the copepod *M. brasilianus*; and for solitary and aggregate life cycle stages of the salps (pelagic tunicates) *Salpa fusiformis* and *S. thompsoni*. Values of  $b_L$  and  $b_R$  were taken or calculated from published data in the sources listed in the electronic supplementary material, where additional data and methodological information can also be found. Values of  $b_A$  for  $\log_{10}$  body SA in relation to  $\log_{10}$  body mass were estimated from  $b_L$  values and scaling exponents of body width versus length (electronic supplementary material). When data for scaling of width versus length were not available, ranges of potential  $b_A$  values are given (based on equations (3.1) and (3.2)). Note the parallel changes in  $b_A$  and  $b_R$  values (shown in italic), regardless of whether decreases or increases in  $b_R$  were observed during ontogeny (except possibly for the transition from veliger larvae to juveniles in *M. edulis*; also see text). Statistically significant ontogenetic shifts in  $b_L$  and  $b_R$  values occur in all species, except for between solitary and aggregate life stages of *S. thompsoni*.

species	stage	$b_L$	$b_A$	$b_R$
<i>Beroe ovata</i>	juveniles	2.92	0.67 (0.67–0.68)	0.62
	adults	2.47	0.80 (0.70–0.81)	0.99
		2.23	0.87 (0.72–0.90)	1.04
		1.78	1.09 (0.78–1.00)	0.86
<i>Aurelia aurita</i>	ephyra larvae	3.14	0.64 (0.64–0.66)	0.63
				0.35
				1.01
	medusae	2.50	0.80 (0.70–0.80)	0.93
		2.72	0.74 (0.68–0.74)	1.11
				1.01
<i>Crassostrea gigas</i>	veliger larvae	2.12	0.95 (0.74–0.94)	0.96
	adults	2.79	0.68–0.72	0.77
<i>Mytilus edulis</i>	veliger larvae	3.49	0.57 (0.57–0.71)	0.90
				0.90
				0.70
				0.59
	juveniles	2.42	0.71–0.83	0.89
	adults	3.17	0.63–0.68	0.66
				0.68
<i>Sagmariasus verreauxi</i>	phyllosoma larvae	2.14	0.91 (0.73–0.93)	1.00
	juveniles	2.99	0.67	0.83
<i>Mesocyclops brasilianus</i>	nauplii	2.15	0.73–0.93	1.08
	copepodites and adults	3.12	0.64–0.68	0.56
<i>Salpa fusiformis</i>	solitary zooids	2.40	0.71–0.83	1.15
	aggregate zooids	2.78	0.68–0.72	0.68
<i>Salpa thompsoni</i>	solitary zooids	2.28	0.72–0.88	0.84
	aggregate zooids	2.41	0.71–0.83	0.92

**Table 2.** Mean ontogenetic scaling exponents from LSRs of  $\log_{10}$  body mass in relation to  $\log_{10}$  body length ( $b_L$ ) and  $\log_{10}$  RMR in relation to  $\log_{10}$  body mass ( $b_R$ ) for nauplii, copepodites and adults of several copepod species ( $b_L$  and  $b_R$  values were taken from published sources given in the electronic supplementary material, whereas the ranges of potential  $b_A$  values for  $\log_{10}$  body SA in relation to  $\log_{10}$  body mass were estimated from  $b_L$  values using equations (3.1) and (3.2) in the text). Mean scaling exponents were calculated by averaging mean conspecific values among species. The 95% CI and number of species sampled ( $n$ ) are given for each scaling exponent. Note the parallel changes in  $b_A$  and  $b_R$  values (shown in italic).

stage	$b_L \pm 95\% \text{ CI } (n)$	$b_A$	$b_R \pm 95\% \text{ CI } (n)$
nauplii	2.28 $\pm$ 0.27 <sup>a</sup> (17)	0.72–0.88	1.00 $\pm$ 0.16 <sup>b</sup> (4)
copepodites and adults	2.84 $\pm$ 0.20 <sup>a</sup> (20)	0.68–0.70	0.72 $\pm$ 0.22 <sup>b</sup> (7)

<sup>a</sup>Based on dry mass, carbon mass or nitrogen mass.

<sup>b</sup>Based on dry body mass.

biphasic or triphasic metabolic scaling appear to be ‘skin-breathers’, i.e. they can absorb oxygen and expel dissolved waste products such as CO<sub>2</sub> through their thin, permeable integuments [39,40]. Some can even absorb nutrients through their body surfaces and metabolize them in their tissues [39,41]. Remarkably, the body-mass scaling slope for metabolism in larvae of the Pacific oyster, *Crassostrea gigas*, is not significantly different from that for uptake of the amino acid alanine [39]. However, it is not known how much cutaneous absorption of nutrients contributes to the overall energy budget of these larvae and other pelagic animals under natural conditions [42]. Our findings point towards the importance of further research on integumentary material exchange by aquatic animals, as a way to better understand variation in their metabolic scaling.

Although parallel shifts in  $b_A$  and  $b_R$  values have usually been seen in this study, possible exceptions invite further scrutiny. For example, although  $b_A$  and  $b_R$  decrease in tandem in the common mussel *Mytilus edulis*, as juveniles mature into adults, more research is needed to determine whether shifts in SA and metabolic scaling also match as veliger larvae develop into juveniles. This is because, although the inferred  $b_A$  shift from 0.57 to 0.71–0.83 parallels the shift of  $b_R$  from 0.77 (based on an average of four values) to 0.89, the individual  $b_R$  estimates for veligers are highly variable, ranging from 0.59 to 0.90 (table 1). Some of this variation appears to be related to temperature, because as temperature increases from 6 to 18°C,  $b_R$  decreases from 0.90 to 0.59 (see the electronic supplementary material), as predicted by the metabolic-level boundaries hypothesis [12]. Sampling error may also be important because the body-size range of growing veligers is small (less than 2 orders of magnitude), thus potentially increasing variation in  $b_R$  estimates [35,43,44] relative to those of juveniles and adults with larger body-size ranges (more than 3 and 4 orders of magnitude, respectively; see electronic supplementary material, table S1). A similar explanation may apply to the variable  $b_R$  estimates (0.35 and 1.01) for two ephyra samples of the scyphozoan *Aurelia aurita* that have body-size ranges less than 1.5 orders of magnitude and that deviate markedly from the inferred  $b_A$  value of 0.64 (table 1). By contrast, the  $b_R$  estimate (0.63) for a third sample of ephyra larvae, with a larger body-size range (more than 2 orders of magnitude), is very close to the estimated  $b_A$  value. Moreover, the  $b_R$  value (0.65) for ephyra larvae of *A. aurita*, estimated from the metabolic data of several studies taken together, is also not significantly different from the inferred  $b_A$  value of 0.64 [45]. It is also possible that our simple Euclidean estimates of SA scaling ( $b_A$ ) do not adequately represent the ontogenetic SA changes occurring in a mussel veliger or an ephyra larva. A veliger’s velum (foot), which has an extensive, highly permeable surface [39], can extend far beyond the measured shell length used in calculating  $b_L$  and  $b_A$  [46]. In addition, the ephyra larva shows complex changes in body shape as it grows, thus making it difficult to accurately estimate the scaling of its SA using our method based on Euclidean geometry (see footnote 7 in electronic supplementary material, table S1).

Another major pattern evident in our results is that, although  $b_R$  is significantly correlated with  $b_A$ , it is usually greater than that predicted by  $b_A$  alone (see tables 1 and 2, and figures 1a,b and 2). Two major factors may help account for these upward deviations of  $b_R$ . First, metabolically costly

growth throughout ontogeny may elevate  $b_R$  values, as has been observed in other animals and plants [3–7,11,23,47]. These growth effects prompt the question: what are the relative influences of resource supply versus metabolic demand by growth and other biological processes on ontogenetic metabolic scaling [4,9–13]? For example, does the steep scaling of SA (and presumably resource uptake) of many kinds of pelagic animals (including larvae) documented here and by Hirst *et al.* [8] permit or even drive the steep scaling of metabolism, or is steep SA scaling a secondary adjustment to steep metabolic scaling that is driven by high resource demand (e.g. mass-specific growth rates that often continue at a high rate throughout ontogeny in pelagic animals [4,48,49])? Attempting to answer this critical question brings into focus the importance of understanding the various factors influencing all of the steps of energy flow through an organism, and their integration, as a way to improve our knowledge of how and why metabolic rate varies with body size (also see [4]).

A second major factor that may help to explain apparent upward deviations in  $b_R$  from that predicted by our SA model (figure 1a) is that we may have underestimated SA changes during ontogeny in our study species. Our geometric estimates of  $b_A$  based on  $b_L$  do not allow the detection of increases in SA related to increased convolutions (or fractal dimensionality) of the body surface, or to the development of special respiratory and nutrient-absorption structures (e.g. the velum in veligers, and the gills in other larval or juvenile forms). In addition, half of our inferred  $b_A$  values (see table 1) may have been underestimated because they were based on the midpoint of a potential range of values, whereas in most cases the upper limit of this range, which involves shape flattening, is probably closer to the actual  $b_A$  value than the lower limit, which involves shape elongation (also see §3 and [8]). This claim is supported by two observations. First, when data on both  $b_L$  and the scaling of body width versus length were available (electronic supplementary material), the inferred  $b_A$  value was almost always closer (in nine of 10 cases) to the predicted upper limit involving mainly two-dimensional growth (flattening) than the lower limit involving mainly one-dimensional growth (elongation) (see table 1). Second, the mean empirical relationship between  $b_L$  and  $b_R$  (and by association  $b_A$ : see figure 2a–c) for all of our study species more closely parallels the slope of the upper predicted boundary involving flattening than that of the lower boundary involving elongation (figure 1b).

Other data consistent with effects of ontogenetic shifts in body shape and SA scaling on metabolic scaling include significant correlations between  $b_L$  and  $b_R$  values among diverse ‘skin-breathing’ pelagic animals, for which species-specific values also show a closer match to the upper boundary curve for predicted  $b_A$  than to the lower boundary curve [8], and parallel steep scaling of SA and metabolic rate in echinoid larvae [50] and epipelagic squid [51]. Steep (often near isometric) scaling of metabolic rate in larval fishes may not only be related to their sustained rapid growth rates [4], but also to their ability to absorb oxygen (and possibly nutrients, though rarely observed) through their entire body surface [52,53]. In addition, shifts from isometric to negatively allometric metabolic scaling seen in plants may be related, at least in part, to decreases in their relative ‘leafiness’ (i.e. reductions in the relative contribution of high SA leaves to total biomass) as they grow [6].



## 6. Conclusion

Ontogenetic shifts in metabolic scaling may often be linked to developmental changes in body shape and SA scaling. Our SA model predicts that this should happen in any organism that relies heavily on body surfaces for resource uptake, such as many kinds of thin-skinned pelagic animals and leafy plants. Ontogenetic shifts in metabolic scaling in other organisms with impermeable integuments may be related to shifts in the SA scaling of specialized respiratory structures (as occur for gills in developing fish [52] and for tracheae during moulting in insect larvae [13]) or to other metabolically demanding developmental changes unrelated to body shape (e.g. shifts from ectothermy to endothermy in developing mammals [4]). Nevertheless, evidence reported here and elsewhere (including near 2/3-power interspecific scaling of basal and cold-induced metabolic rates in birds and small mammals with closed circulatory systems [37]) suggests that the effect of external SA on metabolic scaling may often outweigh or modify the influence of RTNs [4,8,12,47,50,51], contrary to currently influential general



models [1,2]. New resource-transport theory is needed that can accommodate organisms that distribute resources from external surfaces rather than from (or in addition to) internal hubs or 'pumps' (e.g. heart and stomach; also see [8]). More generally, our work and a recent review [47] suggest that a comprehensive explanation of the wide diversity of metabolic scaling relationships that have been observed must consider multiple mechanisms, including those related to SA, all of which have variable effects depending upon taxon, environment and physiological state.

**Acknowledgements.** We thank Andrew Kerkhoff for useful discussions, Mark Jensen for access to his raw data on metabolic rates in the spiny lobster *S. verreauxi*, and Peter Girguis and two anonymous reviewers for helpful comments.

**Funding statement.** D.S.G. was supported by a sabbatical leave granted by Juniata College, A.G.H. was supported by the Natural Environment Research Council and Department for Environment, Food and Rural Affairs (grant no. NE/L003279/1, Marine Ecosystems Research Programme) and D.A. was supported by a Leverhulme Trust Fellowship.

## References

- West GB, Brown JH, Enquist BJ. 1997 A general model for the origin of allometric scaling laws in biology. *Science* **276**, 122–126. (doi:10.1126/science.276.5309.122)
- Banavar JR, Moses ME, Brown JH, Damuth J, Rinaldo A, Sibly RM, Maritan A. 2010 A general basis for quarter-power scaling in animals. *Proc. Natl Acad. Sci. USA* **107**, 15 816–15 820. (doi:10.1073/pnas.1009974107)
- Riisgård HU. 1998 No foundation of a '3/4 power scaling law' for respiration in biology. *Ecol. Lett.* **1**, 71–73. (doi:10.1046/j.1461-0248.1998.00020.x)
- Glazier DS. 2005 Beyond the '3/4-power law': variation in the intra- and interspecific scaling of metabolic rate in animals. *Biol. Rev.* **80**, 611–662. (doi:10.1017/S1464793105006834)
- Czarnoleski M, Kozłowski J, Dumiot G, Bonnet J-C, Mallard J, DuPont-Nivet M. 2008 Scaling of metabolism in *Helix aspersa* snails: changes through ontogeny and response to selection for increased size. *J. Exp. Biol.* **211**, 391–399. (doi:10.1242/jeb.013169)
- Peng Y, Niklas KJ, Reich PB, Sun S. 2010 Ontogenetic shift in the scaling of dark respiration with whole-plant mass in seven shrub species. *Funct. Ecol.* **24**, 502–512. (doi:10.1111/j.1365-2435.2009.01667.x)
- Kutschera U, Niklas KJ. 2011 Ontogenetic changes in the scaling of cellular respiration with respect to size among sunflower seedlings. *Plant Signal. Behav.* **6**, 72–76. (doi:10.4161/psb.6.1.14001)
- Hirst AG, Glazier DS, Atkinson D. 2014 Body shape shifting during growth permits tests that distinguish between competing geometric theories of metabolic scaling. *Ecol. Lett.* **17**, 1274–1281. (doi:10.1111/ele.12334)
- Darveau C-A, Suarez RK, Andrews RD, Hochachka PW. 2002 Allometric cascade as a unifying principle of body mass effects on metabolism. *Nature* **417**, 166–170. (doi:10.1038/417166a)
- Hofmeyr JHS, Rohwer JM. 2011 Supply-demand analysis: a framework for exploring the regulatory design of metabolism. *Methods Enzymol.* **500**, 533–554. (doi:10.1016/B978-0-12-385118-5.00025-6)
- Glazier DS. 2013 Is metabolic rate a universal 'pacemaker' for biological processes? *Biol. Rev.* (doi:10.1111/brv.12115)
- Glazier DS. 2010 A unifying explanation for diverse metabolic scaling in animals and plants. *Biol. Rev.* **85**, 111–138. (doi:10.1111/j.1469-185X.2009.00095.x)
- Callier V, Nijhout HF. 2012 Supply-side constraints are insufficient to explain the ontogenetic scaling of metabolic rate in the Tobacco Hornworm, *Manduca sexta*. *PLoS ONE* **7**, e45455. (doi:10.1371/journal.pone.0045455)
- Rubner M. 1883 Über den Einfluss der Körpergrösse auf Stoff- und Kraftwechsel. *Zeit. Biol.* **19**, 535–562.
- Okie JG. 2013 General models for the spectra of surface area scaling strategies of cells and organisms: fractality, geometric dissimilitude, and internalization. *Am. Nat.* **181**, 421–439. (doi:10.1086/669150)
- West GB, Brown JH, Enquist BJ. 1999 The fourth dimension of life: fractal geometry and allometric scaling of organisms. *Science* **284**, 1677–1679. (doi:10.1126/science.284.5420.1677)
- Dodds PS. 2010 Optimal form of branching supply and collection networks. *Phys. Rev. Lett.* **104**, 048702. (doi:10.1103/PhysRevLett.104.048702)
- Kooijman SALM. 2010 *Dynamic energy budget theory for metabolic organization*. Cambridge, UK: Cambridge University Press.
- Maino JL, Kearney MR, Nisbet RM, Kooijman SALM. 2014 Reconciling theories of metabolic scaling. *J. Anim. Ecol.* **83**, 20–29. (doi:10.1111/1365-2656.12085)
- Savage VM, Deeds EJ, Fontana W. 2008 Sizing up allometric scaling theory. *PLoS Comp. Biol.* **4**, e1000171. (doi:10.1371/journal.pcbi.1000171)
- Price CA *et al.* 2012 Testing the metabolic theory of ecology. *Ecol. Lett.* **15**, 1465–1474. (doi:10.1111/j.1461-0248.2012.01860.x)
- Kleiber M. 1932 Body size and metabolism. *Hilgardia* **6**, 315–353. (doi:10.3733/hilg.v06n11p315)
- Glazier DS, Butler EM, Lombardi SA, Deptola TJ, Reese AJ, Satterthwaite EV. 2011 Ecological effects on metabolic scaling: amphipod responses to fish predators in freshwater springs. *Ecol. Monogr.* **81**, 599–618. (doi:10.1890/11-0264.1)
- Kearney MR, White CR. 2012 Testing metabolic theories. *Am. Nat.* **180**, 546–565. (doi:10.1086/667860)
- Zeuthen E. 1953 Oxygen uptake as related to body size in organisms. *Q. Rev. Biol.* **28**, 1–12. (<http://www.jstor.org/stable/2810299>)
- Kinoshita J, Hiromi J, Kadota S. 1997 Do respiratory metabolic rates of the scyphomedusa *Aurelia aurita* scale isometrically throughout ontogeny in a sexual generation? *Hydrobiologia* **347**, 51–55. (doi:10.1023/A:1002942806113)
- Svetlichny LS, Abolmasova GI, Hubareva ES, Finenko GA, Bat L, Kideys AE. 2004 Respiration rates of *Beroe ovata* in the Black Sea. *Mar. Biol.* **145**, 585–593. (doi:10.1007/s00227-004-1336-4)
- Hirst AG. 2012 Intra-specific scaling of mass to length in pelagic animals: ontogenetic shape change and its implications. *Limnol. Oceanogr.* **57**, 1579–1590. (doi:10.4319/lo.2012.57.5.1579)

29. Glazier DS. 2013 Log-transformation is useful for examining proportional relationships in allometric scaling. *J. Theor. Biol.* **334**, 200–203. (doi:10.1016/j.jtbi.2013.06.017)
30. Jensen MA, Fitzgibbon QP, Carter CG, Adams LR. 2013a Effect of body mass and activity on the metabolic rate and ammonia-N excretion of the spiny lobster *Sagmariasus verreauxi* during ontogeny. *Comp. Biochem. Physiol. A* **166**, 191–198. (doi:10.1016/j.cbpa.2013.06.003)
31. Jensen MA, Fitzgibbon QP, Carter CG, Adams LR. 2013b The effect of stocking density on growth, metabolism and ammonia-N excretion during larval ontogeny of the spiny lobster *Sagmariasus verreauxi*. *Aquaculture* **376–379**, 45–53. (doi:10.1016/j.aquaculture.2012.10.033)
32. DeLong JP, Okie JG, Moses ME, Sibly RM, Brown JH. 2010 Shifts in metabolic scaling, production and efficiency across major evolutionary transitions of life. *Proc. Natl Acad. Sci. USA* **107**, 12 941–12 945. (doi:10.1073/pnas.1007783107)
33. Reiber CL, McGaw IJ. 2009 A review of the ‘open’ and ‘closed’ circulatory systems: new terminology for complex invertebrate circulatory systems in light of current findings. *Int. J. Zool.* **2009**, 301284. (doi:10.1155/2009/301284)
34. McMahon BR, Wilkens JL, Smith PJS. 2011 Invertebrate circulatory systems. *Compr. Physiol.* **2**, 931–1008. (doi:10.1002/cphy.cp130213) 
35. Bokma F. 2004 Evidence against universal metabolic allometry. *Funct. Ecol.* **18**, 184–187. (doi:10.1111/j.0269-8463.2004.00817.x)
36. White CR, Phillips NF, Seymour RS. 2006 The scaling and temperature dependence of vertebrate metabolism. *Biol. Lett.* **2**, 125–127. (doi:10.1098/rsbl.2005.0378)
37. Glazier DS. 2008 Effects of metabolic level on the body-size scaling of metabolic rate in birds and mammals. *Proc. R. Soc. B* **275**, 1405–1410. (doi:10.1098/rspb.2008.0118)
38. Killen SS, Atkinson D, Glazier DS. 2010 The intraspecific scaling of metabolic rate with body mass in fishes depends on lifestyle and temperature. *Ecol. Lett.* **13**, 184–193. (doi:10.1111/j.1461-0248.2009.01415.x)
39. Manahan DT. 1990 Adaptations by invertebrate larvae for nutrient acquisition from seawater. *Am. Zool.* **30**, 147–160. (doi:10.1093/icb/30.1.147)
40. Haond C, Charmantier G, Flik G, Bonga SE. 2001 Identification of respiratory and ion-transporting epithelia in the phyllosoma larvae of the slipper lobster *Scyllarus arctus*. *Cell Tissue Res.* **305**, 445–455. (doi:10.1007/s004410100405)
41. Rodriguez Souza JC, Strüssmann CA, Takashima F, Satoh H, Sekine S, Shima Y, Matsuda H. 2010 Oral and integumental uptake of free exogenous glycine by the Japanese spiny lobster *Panulirus japonicus* phyllosoma larvae. *J. Exp. Biol.* **213**, 1859–1867. (doi:10.1242/jeb.040030)
42. Gomme J. 2001 Transport of exogenous organic substances by invertebrate integuments: the field revisited. *J. Exp. Zool.* **289**, 254–265. (doi:10.1002/1097-010X(20010401/30)289:4<254::AID-JEZ6>3.0.CO;2-F)
43. White CR, Seymour RS. 2005 Sample size and mass range effects on the allometric exponent of basal metabolic rate. *Comp. Biochem. Physiol. A* **142**, 74–78. (doi:10.1016/j.cbpa.2005.07.013)
44. Moses ME, Hou C, Woodruff WH, West GB, Nekola JC, Zuo W, Brown JH. 2008 Revisiting a model of ontogenetic growth: estimating model parameters from theory and data. *Am. Nat.* **171**, 632–645. (<http://www.jstor.org/stable/10.1086/587073>) 
45. Gambill M, Peck MA. 2014 Respiration rates of the polyps of four jellyfish species: potential thermal triggers and limits. *J. Exp. Mar. Biol. Ecol.* **459**, 17–22. (doi:10.1016/j.jembe.2014.05.005)
46. Hamburger K, Møhlenberg F, Randløv A, Riisgård HU. 1983 Size, oxygen consumption and growth in the mussel *Mytilus edulis*. *Mar. Biol.* **75**, 303–306. (doi:10.1007/BF00406016)
47. Glazier DS. 2014 Metabolic scaling in complex living systems. *Systems* **2**, 451–540. (doi:10.3390/systems2040451)
48. Glazier DS. 2006 The 3/4-power law is not universal: evolution of isometric, ontogenetic metabolic scaling in pelagic animals. *Bioscience* **56**, 325–332. (doi:10.1641/0006-3568(2006)56[325:TPLINU]2.0.CO;2)
49. Hirst AG, Forster J. 2013 When growth models are not universal: evidence from marine invertebrates. *Proc. R. Soc. B* **280**, 20131546. (doi:10.1098/rspb.2013.1546)
50. McEdward LR. 1984 Morphometric and metabolic analysis of the growth and form of an echinopluteus. *J. Exp. Mar. Biol. Ecol.* **82**, 259–287. (doi:10.1016/0022-0981(84)90109-6)
51. Seibel BA. 2007 On the depth and scale of metabolic rate variation: scaling of oxygen consumption rates and enzymatic activity in the Class Cephalopoda (Mollusca). *J. Exp. Biol.* **210**, 1–11. (doi:10.1242/jeb.02588)
52. Post JR, Lee JA. 1996 Metabolic ontogeny of teleost fishes. *Can. J. Fish. Aquat. Sci.* **53**, 910–923. (doi:10.1139/f95-278)
53. Glover CN, Bucking C, Wood CM. 2013 The skin of fish as a transport epithelium: a review. *J. Comp. Physiol. B* **183**, 877–891. (doi:10.1007/s00360-013-0761-4)
54. Cumming G. 2008 Inference by eye: reading the overlap of independent confidence intervals. *Stat. Med.* **28**, 205–220. (doi:10.1002/sim.3471)